 IEEE Transactions on Nuclear Science, Vol. NS-30, No. 4, August 1983

CW SIDE-COUPLED LINAC FOR THE LOS ALAMOS/NBS RACETRACK MICROTRON*

L. M. Young and J. M. Potter, AT-1. MS H817
Los Alamos National Laboratory, Los Alamos, NM 87545

Summary

A 2.7-m side-coupled linac has been built as part of the 5-MeV injector for the cw room-temperature racetrack microtron (RTM) being constructed in collaboration with the National Bureau of Standards (NBS).[1] The linac is designed to accelerate the electron beam from 1 to 5 MeV with an accelerating gradient of 1.5 MeV/m. Fabrication of the structure started October 4, 1982 and was completed February 28, 1983, when it was tested with a cw power level of 82 kW. The structure has an effective shunt impedance (ZT^2) of 82.5 MΩ/m. No change in field distribution was detected at any power level. The operating frequency is 2380 MHz.

Introduction

Four different types of standing-wave, coupled-cavity rf linear accelerator structures have been investigated in a search for the best candidates for the RTM: disk-and-washer (DAW), annular-ring coupled structure (ACS), on-axis coupled structure (OCS), and side-coupled structure (SCS).[2] Our goal has been to develop a structure with five properties: (1) a high efficiency ($ZT^2 \geq 80$ MΩ/m) to reduce the rf power consumption; (2) an ability to support high accelerating fields ($\geq$1.5 MeV/m); (3) sufficient water cooling to permit 100% duty factor operation; (4) freedom from interfering modes that could cause beam breakup or could compromise structure efficiency; (5) enough coupling ($\geq$10%) to ensure good stability with long assemblies of many cells to optimize match to rf amplifier size.

From our studies, we conclude that an advanced SCS structure with 5% coupling would meet objectives in Items 1-4 but would not be optimum for the objective in Item 5. However, 5% coupling is adequate for 4-m-long structures at 2380 MHz. Therefore, the RTM requirements can be met by using two 4-m structures to provide the 8 m of accelerating structure needed.

The recently completed 2.7-m section meets our design objectives. The shunt impedance is 82.5 MΩ/m, which satisfies Goal 1. After we conditioned the structure for 3 h, it accepted 82 kW of cw rf power, corresponding to a 1.58-MeV/m accelerating gradient. This power level was achieved with only 70% of the design water flow; thus, Goals 2 and 3 are satisfied. Goal 4 is satisfied because no interfering modes are found near the operating frequency f_0. The lowest beam-blowup modes occur in a band between 3/2 f_0 and 2 f_0, which avoids ratios of small integers. Therefore, no serious problem is expected with these modes. Goal 5 is satisfied to the extent that the 2.7-m structure has a 0.048 coupling factor and is stable at least up to 30 kW/m. No power-induced field tilt was observed. Field distribution has an rms amplitude fluctuation about the mean of 2.1% and a <0.5% field tilt. The stop band, which was preset to +400 kHz to avoid thermal runaway that is possible with a negative stop band, increased with power at a rate of 12 kHz/kW/m to a value of +770 kHz at 30 kW/m. Thus, there is no possibility of the stop band going negative at higher power levels. The frequency of the accelerating mode drops at a rate of 21 kHz/kW/m with increasing power levels when water temperature remains constant. To maintain constant frequency, the water temperature must be reduced as power is increased.

The 2380-MHz Side-Coupled Structure

For the free-electron-laser/LAMPF cell geometry scaled to the RTM 2380-MHz frequency, the predicted ZT^2, including losses from surface finish, is 70 MΩ/m. This is unacceptably low, both because of length constraints imposed by available space at NBS and because of klystron power limitations. A study of shunt impedance versus parameters made for LAMPF suggests that slight improvements to the shunt impedance could be made by decreasing the beam aperture and by sharpening the nose angle of the cavity (see Fig. 1).[3] The desired beam aperture size is 1 cm, which is 78% of the scaled LAMPF beam hole. The nose angle was decreased from 30 to 10°. This decrease, together with the reduction in beam aperture, increased the theoretical shunt impedance by 18%, to 99 MΩ/m. The peak surface field is still well below the Kilpatrick limit. The actual measured shunt impedance in the 2.7-m structure for the RTM program is 82.5 ± 1 MΩ/m. The reduction from theoretical is due entirely to decreased Q because of surface-finish effects and redistribution of current by the coupling slots. The measured value of ZT^2/Q, which is independent of cavity Q, was within 1% of the SUPERFISH value, 5397 Ω/m.

The unloaded Q (Q_μ) measurement for the almost completely brazed structure (only the drive cell was not brazed) yielded a 15 300 Q compared to the 18 340 SUPERFISH value. The loaded Q (Q_ℓ) was measured after the iris was cut with a match of ß = 1.04. Q_ℓ is related to Q_μ by the relation

$$Q_\ell = \frac{Q_\mu}{1 + \beta} \quad .$$

The Q measurements, made before and after the iris slot was cut, agreed within 1% using this relation. The measured values of Q and ZT^2/Q yield 82.5 MΩ/m for the shunt impedance, ZT^2.

Using a least squares fit of the measured mode spectrum to the predicted mode spectrum, we calculated the derived parameters of the SCS, given in Table I, from the coupled-circuit model.[4] The measured mode spectrum was obtained from the 2.7-m section consisting of 43 accelerating cells and 42 coupling cells.

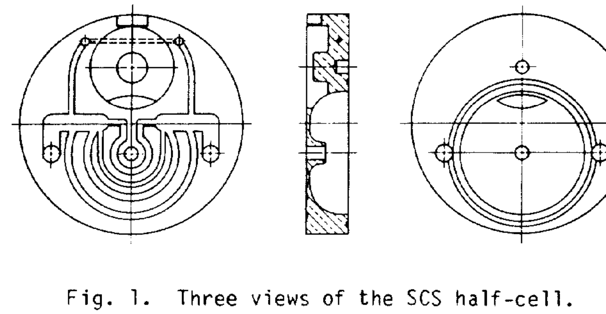

Fig. 1. Three views of the SCS half-cell.

*Work supported by US Department of Energy.

0018-9499/83/0800-3508$01.00© 1983 IEEE

Estimates of power-flow droop, power-flow phase shift, and tilt sensitivity can be made using the coupled-circuit model. For the rf drive in the center of the 2.7-m SCS with the parameters given in Table I, the estimated power-flow droop from the center to each end is 0.3%. The power-flow phase shift is 0.5° for a 400-kHz stop band. Under full power when the stop band is 770 kHz, the power-flow phase shift increases to 1.0°. The tilt sensitivity (tilt produced by deliberately detuning the end cells equally and oppositely) is 1%/MHz of end-cell detuning for the 400 kHz stop band and 2%/MHz for the full-power 770-kHz stop band.

Using SCRAM (a program that solves the general coupled-circuit model), we have determined semi-empirically that the rms amplitude fluctuation is $\sigma = 11\ N/K^2(d\omega/\omega_{\pi/2})_{rms} \cdot (d\omega_s/\omega_{\pi/2})$, where N is the number of accelerating cells, K is the nearest neighbor coupling constant, $(d\omega/\omega_{\pi/2})_{rms}$ is the relative rms deviation of cell frequencies, and $(d\omega_s/\omega_{\pi/2})$ is the relative stop-band width. For the parameters in Table I, $\sigma = 0.2\%$. This effect is much smaller than the effect of coupling-constant errors. The effect of errors in coupling constant on the field

TABLE I

PARAMETERS OF THE SIDE-COUPLED STRUCTURE

Measured Parameters	
Operating frequency	2380 MHz
Standard deviation of accelerating cell frequencies excluding the two end cells, which are tuned ~2.1 MHz lower[a]	200 kHz
Standard deviation of coupling-cell frequencies[a]	28 kHz
Q_A, accelerating-cell Q	15 300
Q_C, coupling-cell Q	7500
ZT^2, effective shunt impedance	82.5 MΩ/m
Derived Parameters	
Accelerating-cell frequency	2387.0 MHz
Coupling-cell frequency	2378.4 MHz
Nearest neighbor coupling constant K	0.0476
Direct coupling between accelerating cells K_A	-0.006
Direct coupling between coupling cells K_C	0.0015
Stop band[b]	0.296 MHz

[a] The standard deviation of cell frequencies are from measurements made of cell frequencies during tuning.

[b] The stop band given in the table is derived from the fit to all the modes, whereas the stop band values given in the text are determined from only three modes: the accelerating mode and the two nearest modes that couple to the structure drive. The two modes next to the accelerating mode do not couple to the structure drive and therefore cannot be used to determine the stop band when the structure is under power.

distribution of resonantly coupled accelerator structures also can be predicted using the coupling-circuit model. If the two coupling constants from a coupling cell to the accelerating cells on each side of it are not matched, the amplitude ratio of the two accelerating fields will be the inverse of the corresponding coupling-constant ratio. Because this effect is cumulative, a small systematic error in the coupling-constant ratio can result in significant tilt if it continues over many cells. For example, if the coupling constants are consistently unbalanced by 0.5%, the field tilt will be 16% over 32 cells. Random fluctuations of 0.5% are not significant. The solution to this potential problem is to assemble the structure before brazing and measure its field distribution by the bead-pull technique. Any tendency for coupling-constant errors to accumulate can be counteracted by reversing some of the cells so that the coupling errors tend to cancel each other.

The structure was assembled before brazing, and the field distribution was measured by the bead-pull technique. The ordering of the cells then was changed to counteract the field tilts caused by the coupling-constant errors. The field fluctuations that remained after this process essentially were unchanged by the subsequent brazing and tuning operations. When first clamped together, the structure had a 5% maximum rms amplitude fluctuation, and the first half of the structure had an average amplitude ~8% greater than the second half; whereas, after reordering, brazing, tuning, and final assembly, the difference was only 0.4% between the first and second half with only 2.1% rms amplitude fluctuation. This improvement in the field distribution (see Fig. 2) illustrates the power of the reordering technique.

Construction

The small size of this structure permits a half-accelerating-cell and a half-coupling-cell to be made from a monolithic copper piece (see Fig. 1). Two of these pieces and a stainless steel vacuum port are brazed together in a single heat to form water channels in the septum and a coupling cell with vacuum port. The braze alloy used for this braze is 65% silver, 15% palladium, and 20% copper with a 1652°F liquidus. Good results have been obtained with this alloy in making the copper-to-copper and copper-to-stainless-steel braze at 1710° ± 10°F. (Poor results were obtained using this alloy at 1760°F on the copper-to-copper joints, which appeared to be porous when vacuum leak checking was performed.) These assemblies then are brazed together with 72% silver, 28% copper braze alloy with 1436°F liquidus to form sections of the accelerator ~1 m long. These sections have flanges on the end so they can be bolted together to form a complete accelerator section.

The integral monolithic half-cell design is well suited to cooling. Water passages have been designed

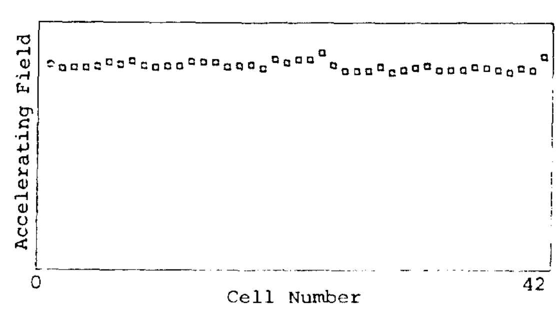

Fig. 2. Field distribution of preaccelerator structure obtained from bead-pull data. Vertical scale is arbitrary.

to apportion water flow to minimize temperature gradients. These designs are depicted in Fig. 1. These water passages are based on 2.56 gpm/cell and a velocity not in excess of 12 ft/s.

The machining-finish roughness for all inner contours has been set at 63-rms-microinch roughness, maximum. This finish is attainable with "off-the-shelf" carbide insert-type tools that normally are used for tracer lathe machining. Some surfaces were checked by profilometer and found to be in the 51- to 58-rms-microinch range. This seems to be the range of surface finish that can be expected of commercially ground tool inserts. Measurements on a single, brazed cell with no coupling slots, machined with this method, yielded a Q value of 17 800 at 2380 MHz, which is 95% of theoretical.

Accelerating and coupling half-cells are tuned in place on a lathe to within 300 kHz and 1 MHz, respectively, by machining to an accuracy of approximately ±0.0003 in. The frequency to which the cells are tuned has been estimated to correct for the effects of vacuum and temperature on the assembled structure and the desired stop band. Final tuning of the accelerating cells after brazing is accomplished by deforming the cell walls slightly at access points provided by drilling the structure to reduce the wall thickness at four locations on each cell. The accelerating cell frequencies can be only raised: whereas, the coupling cells can be lowered by squeezing the gap or raised by spreading the gap with a wedge. For this reason, in the lathe the accelerating cells are tuned ~300 kHz lower than required. To obtain the desired operating frequency, the final tuning of the accelerating cells requires the cells only to be raised in frequency.

Coupling Iris

A short brazed section was used to determine the approximate size of the coupling iris required for a full-length accelerator section. The coupling factor β_2, obtained when a structure has N_2 accelerating cells of $Q = Q_2$ when the coupling factor is β_1 for a geometrically identical structure of N_1 accelerating cells of $Q = Q_1$, is

$$\beta_2 = \beta_1 \frac{Q_2}{Q_1} \frac{N_1}{N_2} \quad ,$$

assuming the fields are uniformly distributed in each case.

The product $\beta_2 \cdot N_2$ for $Q_2 = 15\,000$ is plotted in Fig. 3. The solid line represents data from the six-cell test cavity. The + represents the data obtained from cutting the iris on the preaccelerator. The iris was 13 mm wide on the six-cell test cavity, and the edges were left square; whereas, on the preaccelerator, the iris was 9.5 mm wide with all edges rounded off. The length of the slot has the predominent effect on the coupling. The slot width virtually has no effect. The fact that the edges were rounded on the preaccelerator coupling iris probably accounts for the slightly greater coupling than that observed with the test cavity.

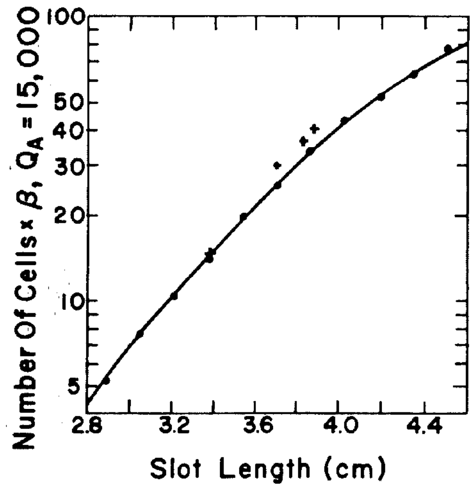

Fig. 3. Coupling factor versus iris slot length.

Acknowledgments

The authors would like to thank W. L. Clark, R. F. DePaula, and F. A. Martinez for the long hours of work machining and assembling the side-coupled structure so quickly. Also, we would like to thank L. C. Wilkerson, P. L. Roybal, D. J. Kennedy, P. B. Bradley, K. J. Lovell, and J. F. Martinez for their participation in either designing, drafting, or brazing of the structure. Finally, we would like to thank F. J. Humphry for help with the bead-pull measurements.

References

1. P. H. Debenham, S. Penner, R. L. Ayres, R. I. Cutler, E. R. Lindstrom, D. L. Mohr, J. E. Rose, M. A. D. Wilson, and N. R. Yoder; L. M. Young, E. R. Martin, A. Mitra, J. M. Potter, R. H. Stokes, P. J. Tallerico, and L. Wilkerson, "Progress on the NBS-LANL CW Microtron," IEEE Trans. Nucl. Sci. 30, No. 2, to be published April 1983.

2. R. K. Cooper, Y. Iwashita, J. M. Potter, S. O. Schriber, D. A. Swenson, J. M. Watson, L. C. Wilkerson, and L. M. Young, "Radio-Frequency Structure Development for the Los Alamos/NBS Racetrack Microtron," Los Alamos National Laboratory document LA-UR-83-95 (January 1983).

3. "Quarterly Status Report on the Medium-Energy Physics Program for the Period Ending April 30, 1967," Los Alamos Scientific Laboratory report LA-3712-MS, p. 8 (May 1967).

4. E. A. Knapp, B. C. Knapp, and J. M. Potter, "Standing-Wave High Energy Linear Accelerator Structure," Rev. Sci. Instrum. 39, p. 979 (1968).